

1 Thermodynamic pedodiversity patterns reveal
2 higher-order soil organization in indigenous
3 agroecosystems of the U.S. Southwest

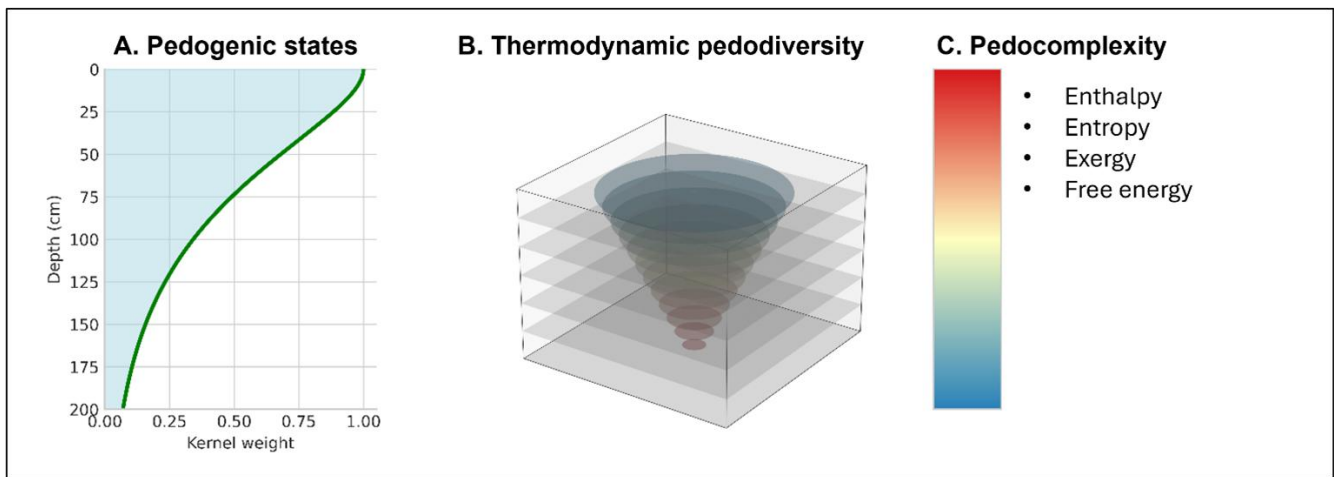
4 Trevan Flynn^{a,b*}

5 ^aDepartment of Agronomy, University of Fort Hare, Alice, 5700 South Africa

6 ^bDepartment of Research, add1Technologies, 11531 Slick Rock Dr., Richmond TX 77406 USA

7

8 Correspondence: t.flynn@add1technologies.com



9

10

11

12

13 Abstract

14 Soil spatial heterogeneity and diversity support the stability and productivity of food systems, yet
15 their multidimensional structure remains difficult to quantify at spatial scales relevant to
16 agricultural resilience. A process-based framework grounded in fundamental physical principles
17 is therefore needed to describe these spatial processes across landscapes. The aim of this study
18 was to develop a mechanistic three-dimensional thermodynamic pedodiversity index constrained
19 by physical continuity. The framework was applied to ancestral and contemporary indigenous
20 agroecosystems of the U.S. Southwest. Eight gridded soil properties were transformed into
21 thermodynamic exergy states using a three-dimensional biweight multi-pass convolution applied
22 across spatial directions, with the surface layer subject to atmospheric forcing. Local inverse
23 Moran's I was then calculated to quantify the pedodiversity patterns. Linking thermodynamic
24 principles to the landscape scale revealed that long-term crop production aligns with structured
25 pedodiversity patterns rather than with pedodiversity magnitude alone. Persistent Hopi dryland
26 agriculture corresponded with moderately to highly organized pedodiversity patterns, whereas
27 more specialized Navajo pastoral systems occurred in landscapes characterized by lower
28 pedodiversity organization. These results suggest that pedodiversity represents only one
29 component of soil resilience and multifunctionality. Higher-order spatial processes, interpreted
30 alongside indigenous ecological knowledge, are necessary to understand how soils support
31 sustained agroecosystems. Integrating process-based applied mathematics with Indigenous
32 knowledge systems may therefore provide a pathway toward identifying higher-order functions
33 capable of inferring soil resilience and multifunctionality.

34 **Keywords:** Exergy, Indigenous knowledge, Soil resilience, Soil multifunctionality, Quantitative
35 pedology

36 1. Introduction

37 Soil is an inherently complex system shaped by the interaction of biological, chemical, physical
38 (Jenny, 1941) and anthropogenic processes that operate across multiple spatial, depth and
39 temporal scales simultaneously (Dearing et al., 2014). These processes generate a remarkable
40 degree of variability both across the landscape and through the soil profile that are essential for
41 ecosystem services such as water regulation, carbon storage and nutrient cycling (McBratney and
42 Minasny, 2007). Understanding soil multifunctionality and resilience requires capturing the
43 variability, a task that remains conceptually and methodologically challenging. The field of
44 pedodiversity emerged to provide a quantitative framework for describing this heterogeneity and
45 connecting it to ecological and pedogenic dynamics (Ibáñez et al., 1995).

46 Classically, pedodiversity has been quantified through the diversity of soil types (taxonomic), soil
47 horizons (genetic) or soil productivity under different environmental changes (functionality)(Ibáñez
48 and Bockheim, 2013). While valuable, these methods are constrained by their reliance on discrete
49 taxonomic boundaries (Zhu, 1997) or rely on one purpose and thus fail to capture the continuous
50 and multidimensional nature of soil variation, the interactions among soil attributes or rely on one
51 attribute which does not reflect the true multifunctionality of soil (Toomanian and Esfandiarpour,
52 2010). Accordingly, there is a need to calculate pedodiversity by recognizing that soil varies not
53 only vertically with depth but also laterally across the landscape, and that processes occurring

54 within one profile can influence the functionality of neighbouring soil and horizons (Matheron,
55 1963).

56 In the U.S. Southwest, soil preserves a long record of interactions between people, agriculture and
57 climate. The Ancestral Pueblo, Navajo and Hopi (among many others) agricultural systems
58 developed under extreme climatic constraints, relying on detailed ecological knowledge and a
59 profound understanding of soil heterogeneity to sustain crop production over centuries during
60 extreme climatic events. For instance, the cultural and trading center of Chaco Canyon likely
61 imported food from the Chuska Mountains to the west, where maize, beans and squash could be
62 cultivated (Benson et al., 2003). In Mesa Verde, agriculture was primarily conducted on the mesa
63 tops and extended northward into the Great Sage Plains, which were extensively cultivated by the
64 late era of the Ancestral Pueblo (Benson, 2011). Yet, it remains unclear whether these lands were
65 chosen for their extensive homogeneous, high-quality soil or for their spatially heterogeneous
66 variation, which may have offered greater adaptive opportunities under varying climatic
67 conditions.

68 The Hopi, considered possible cultural descendants of the Ancestral Pueblo have practiced
69 dryland farming for at least nine centuries, since around 1,100 A.D. (Bocinsky and Varien, 2017),
70 possibly following the decline of Chaco Canyon. Their agricultural system exemplifies an enduring
71 strategy that capitalizes on pedodiversity, intentionally seeking sites that differ from the
72 surrounding landscape to maximize functional diversity and resilience. The Hopi territory
73 represents one of North America's longest-inhabited agricultural landscapes (Johnson, 2023) and
74 a recognized biodiversity hotspot (Nankar and Pratt, 2021), shaped by cultural practices that
75 exploit soil variability, crop diversity through selective breeding and has lasted through extreme
76 drought. For example, the Hopi cultivate 17 distinct drought-resistant nutrient dense maize

77 varieties, an exceptional adaptation given maize's typical dependence on abundant water (Soleri
78 and Cleveland, 1993).

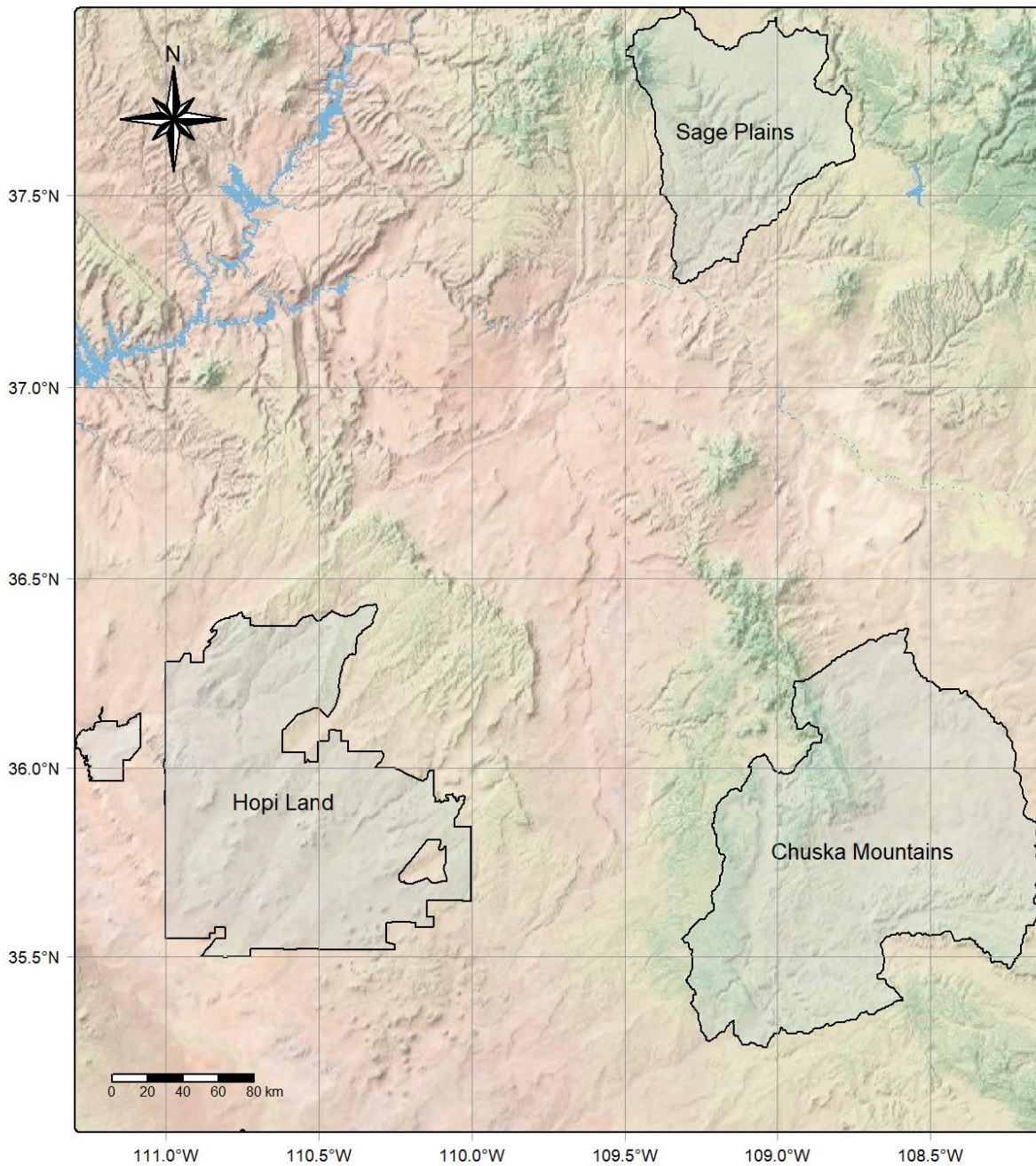
79 By continuously quantifying pedodiversity, we can reveal how this intrinsic, multidimensional soil
80 complexity supports the persistence of traditional dryland farming systems (Mikhailova et al.,
81 2021). High vertical pedodiversity reflects the development of layered soil profiles or profiles with
82 discrete boundaries, whereas spatial pedodiversity represented the by spatial heterogeneity (i.e.,
83 squared differences) of niches historically exploited for distinct crops, breeding and management
84 strategies. Mapping these interconnected domains simultaneously shows landscapes where
85 agricultural traditions have upheld ecological balance and soil functionality across generations
86 (Costantini and L'Abate, 2016). Conversely, such analyses may also reveal agricultural strategies
87 that favored lower pedodiversity and greater soil homogeneity in areas possessing inherently
88 favorable soil and moisture regimes.

89 The aim of this study was to quantify a process-based, numerical second-order voxel index to
90 characterize the pedodiversity of soil thermodynamic states, providing insight into community-
91 level soil behavior. Applied across Ancestral Pueblo agricultural landscapes and multigenerational
92 dryland farming regions of the U.S. Southwest, we show that thermodynamic pedodiversity or soil
93 system organization, forms part of a framework for assessing soil resilience and societal
94 adaptation to environmental stress. By capturing physical properties, spatial structure and depth
95 organization, this approach offers a rigorous measure of soil arrangements and an ecological-
96 cultural perspective for understanding how human management practices have persisted,
97 adapted and transformed under variable environmental conditions.

98 2. Methods and materials

99 2.1 Sites

100 The Four Corners region of the U.S. southwest and the three sites chosen were selected because
101 they represent the agricultural and cultural legacies of the Ancestral Pueblo, Navajo and Hopi
102 peoples (Brooks, 2020) whose histories are interrelated through geography yet are culturally
103 distinct (Figure 1). Although the Navajo and Hopi occupy regions that overlap with former Ancestral
104 Pueblo territories and each other, their languages, cultural practices and agricultural systems
105 differ significantly (Dongoske et al., 1997; Kahn-John (Diné) and Koithan, 2015). For this reason,
106 and in recognition of their unique cultural identities and histories, the Navajo and Hopi are distinct
107 from the Ancestral Pueblo. The cultural history of the region is further complicated by overlapping
108 territorial boundaries; for example, Hope Land lies within the Navajo Nation, yet the two peoples
109 maintain separate cultural traditions. Additionally, the term “Anasazi”, historically used in
110 archaeological literature to refer to the Ancestral Pueblo is now avoided due to its derogatory
111 meaning, “ancient enemy,” (McBrinn and Cordell, 2016) in Diné Bizaad (the Navajo language).
112 Whether this term originated as a Western construct or was relayed to archaeologist Richard
113 Wetherill, who popularized it, remains uncertain, but its use highlights the importance of cultural
114 sensitivity and self-identification in interpreting the human history of the U.S. Southwest.



115

116 *Figure 1: known indigenous lands selected based on borders or basins due to water resources, which likely determined their*
 117 *agriculture practices.*

118 Except for Hopi Land, the sites were delineated primarily from hydrological basins identified
 119 through a digital elevation model (DEM), crossing state boundaries (Colorado, Utah, Arizona and
 120 New Mexico). This geomorphic criterion was chosen because, although some ancestral cultures

121 constructed irrigation networks, all ultimately relied on dryland agriculture (Bellorado and
122 Anderson, 2013). Basins or catchments, concentrate runoff and moisture and thus represent the
123 most probable zones of Ancestral Pueblo cultivation. Site selection also considered the spatial
124 distribution of early and late Ancestral Pueblo agricultural landscapes and their overlap with the
125 territories of contemporary Indigenous peoples. While this spatial correspondence is inherently
126 interpretive, it reflects well-established archaeological and ethnogeographic evidence that the
127 Ancestral Pueblo peoples inhabited and farmed across the Four Corners region of the U.S.
128 Southwest.

129 2.1.1 Chuska Mountains

130 The southern Chuska Mountains, southern basin and its piedmonts, straddling the Arizona–New
131 Mexico border, form a volcanic highland rising above the surrounding Colorado Plateau. The range
132 is composed primarily of Oligocene basaltic and andesitic flows (Appledorn and Wright, 1957),
133 interbedded with volcanoclastic sandstones and Chuska Sandstone, underlain by older Mesozoic
134 sedimentary formations such as the Navajo and Wingate Sandstones. Elevation ranges from
135 approximately 1,800 to 2,900 m, with the southern basin averaging 2,053 m (Blagbrough, 1967).
136 Vegetation transitions sharply from montane forests of ponderosa pine, spruce and fir at higher
137 elevations to pinyon–juniper woodland and semi-arid grassland across the lower slopes and
138 basins (Harris et al., 1960). The climate spans alpine to desert conditions, characterized by cool,
139 snowy winters and warm, dry summers, with precipitation varying from $>500 \text{ mm yr}^{-1}$ on the crest
140 to $<250 \text{ mm yr}^{-1}$ in the southern lowlands (Blagbrough, 1967). Culturally, this region was a critical
141 resource and agricultural hinterland for Chaco Canyon (~900 AD), supplying timber and
142 agricultural products to the Ancestral Pueblo (Wills et al., 2014). The same landscapes are

143 traditional herding and grazing grounds of the Navajo Nation, whose pastoral systems continue to
144 shape soil use and vegetation patterns (Wallace et al., 2021).

145 2.1.2 Great Sage Plain

146 The Great Sage Plains lies north of Mesa Verde and west of the Dolores River in southwestern
147 Colorado and southeastern Utah, forming part of the northern San Juan Basin margin. The
148 landscape consists primarily of Cretaceous Mancos Shale overlain by Quaternary loess, alluvium
149 and colluvial deposits, with minor outcrops of the Dakota Sandstone and Mesa Verde Group along
150 drainage margins (Reheis et al., 2018). The average elevation is 2,050 m, with a gently undulating
151 topography that contrasts sharply with the dissected mesas to the south (Dove et al., 2006). Soil
152 is predominantly fine-textured loams and clay loams, developed on shale and loess parent
153 materials that provide high moisture retention but limited infiltration (Fadem and Diederichs,
154 2020). The regional climate is semi-arid continental, with cold winters, warm summers and mean
155 annual precipitation of 300–400 mm, much of it derived from winter snowmelt. Vegetation is
156 dominated by sagebrush steppe, greasewood and semi-arid grassland, interspersed with dryland
157 agricultural fields (Wagner and Scipal, 2000). Archaeologically, this area marks the northern
158 agricultural frontier of the Ancestral Pueblo world, cultivated most intensively between 1000 and
159 1280 A.D., (Allison, 2010).

160 2.1.3 Hopi Land

161 The Hopi Mesas occupy a prominent series of east–west–oriented uplands in northeastern
162 Arizona, rising above the northern edge of the Little Colorado River Basin. The landscape is
163 underlain by Jurassic and Triassic sandstones, principally the Entrada, Wingate and Navajo
164 Sandstones interbedded with minor siltstone and shale that create subtle contrasts in soil texture

165 and water-holding capacity (O’Sullivan, 2003). Elevation ranges from approximately 1,700 to 1,900
166 m, and the region’s arid to semi-arid climate is characterized by mean annual precipitation of 200–
167 300 mm, concentrated during the summer monsoon, with mean annual temperatures of 10–13 °C
168 (Hopi Department of Natural Resources, 2021). Vegetation is mostly pinyon–juniper woodland,
169 sagebrush and mixed grassland, with riparian shrubs in ephemeral washes. The region forms one
170 of North America’s oldest continuously farmed landscapes, where the Hopi people have practiced
171 dryland agriculture for over nine centuries. Their fields, often situated on mesa slopes and valley
172 bottoms, support a remarkable diversity of drought-tolerant maize, beans, squash, melons and
173 medicinal plants (Johnson et al., 2021; Wall and Masayeva, 2004).

174 2.2 Soil data

175 Soil property data was obtained from the POLARIS (Probabilistic Remapping of SSURGO) dataset
176 (Chaney et al., 2016). and the USDA-NCSS soil survey data (SSURGO back-filled with STATSGO
177 where SSURGO is not available) database (Walkinshaw, 2020), both providing harmonized,
178 gridded soil property estimates across the conterminous United States. POLARIS was used to
179 represent the physical soil matrix, while USDA-NCSS soil survey supplied soil color data critical
180 for redox-morphological interpretation (Kim et al., 2025). All soil properties were obtained within
181 the Google Earth Engine (GEE; Gorelick et al., 2017) to streamline the modelling process.

182 The POLARIS dataset provides probabilistic predictions of major soil attributes at a 30 m spatial
183 resolution (Chaney et al., 2016). Seven properties were extracted for this study: bulk density (g
184 cm^{-3}), sand (% w/w), silt (% w/w), clay (% w/w), saturated hydraulic conductivity (K_{sat} ; $\log_{10}(\text{cm hr}^{-1})$), soil organic matter ($\log_{10}(\% \text{ w/w})$) and pH. Each property was available at the six standard
185 GlobalSoilMap (Arrouays et al., 2014) depth intervals: 0–5, 5–15, 15–30, 30–60, 60–100 and 100–

187 200 cm. All soil properties were retained in their transformed state; for example, K_{sat} and soil
188 organic matter were kept in their \log_{10} -transformed form, as their distributions are typically right-
189 skewed and approximate normal after transformation (Shapiro et al., 1968; Webster and Oliver,
190 2007). This approach also preserves the proportional relationships among properties, which is
191 preferable for kernel-based weighting and correlation analysis (McBratney et al., 1992).

192 Soil color acts as a morphological proxy for oxidation–reduction and drainage conditions, it was
193 included as an eighth property to enhance the interpretability of the pedodiversity index. Munsell
194 soil color data were resampled to 30 m spatial resolution using a nearest-neighbor approach to
195 preserve the native fine-scale texture of the dataset. Depth intervals were retained in their original
196 form, as the 3-dimensional kernel weights were designed to account for cross-layer influence of
197 soil color at 10, 25, 75, and 125 cm.

198 2.3 Thermodynamic pedodiversity

199 2.3.1 Pedocomplexity theory

200 Thermodynamic pedodiversity is a key element of pedocomplexity, a framework that integrates soil
201 thermodynamic states, continuous diversity, total potential energy and practical tools (e.g.,
202 decision-support) to evaluate soil resilience and multifunctionality. It emphasizes that
203 pedodiversity alone cannot serve as a proxy for soil functionality, and that soil multifunctionality is
204 instead governed by pedocomplexity. Pedocomplexity is a function describing the thermodynamic
205 steady-state of soil, from which, using a multidisciplinary approach, soil resilience and
206 multifunctionality can be inferred. Pedocomplexity is comprised of four components (Table 1).

Component	Steady state	Physical meaning
Latent energy	Enthalpy (ΔH)	The total stored energy that is not yet contributing to work.
Pedogenic states	Exergy (Ψ)	The magnitude of internal energy available for work (usable energy in the soil).
Pedogenic exchange	Entropy (σ)	The coupling or interaction energy dissipated to maintain gradients between pedogenic states.
Pedocomplexity	Organization of exergy (O)	A function of H , Ψ and σ describing the thermodynamical structure of the soil system

208

209 When defined for the whole system pedogenic states can be described as magnitude or intensity
 210 and pedogenic exchange can be shown as a thermodynamic pedodiversity index. The framework
 211 recognizes that soil always exists in a multidimensional physical and feature state. However, the
 212 term “pedogenic” is emphasized as a descriptor of process-based functions culminating in
 213 pedocomplexity, calculated as:

214
$$O(s) = \int f: \mathbb{C}(\Delta H, \Psi, \sigma)_{x,y,z,t} dV,$$

215 Or if the data is sparse, non-continuous or simply not enough data:

216
$$O(s) = \int f(\Delta H, \Psi, \sigma)_{x,y,z} dV$$

217 Where latent energy corresponds to enthalpy ΔH , representing total stored energy in a form that
 218 that is not is not capable to perform work. Pedogenic states are equivalent to exergy Ψ , capturing
 219 the usable internal energy available for work. Pedogenic exchange acts like entropy σ , representing
 220 the interaction energy dissipated to maintain spatial gradients between states. Finally,
 221 pedocomplexity (O) is a function of ΔH , Ψ and σ , describing the overall thermodynamic structure
 222 of the soil system organization.

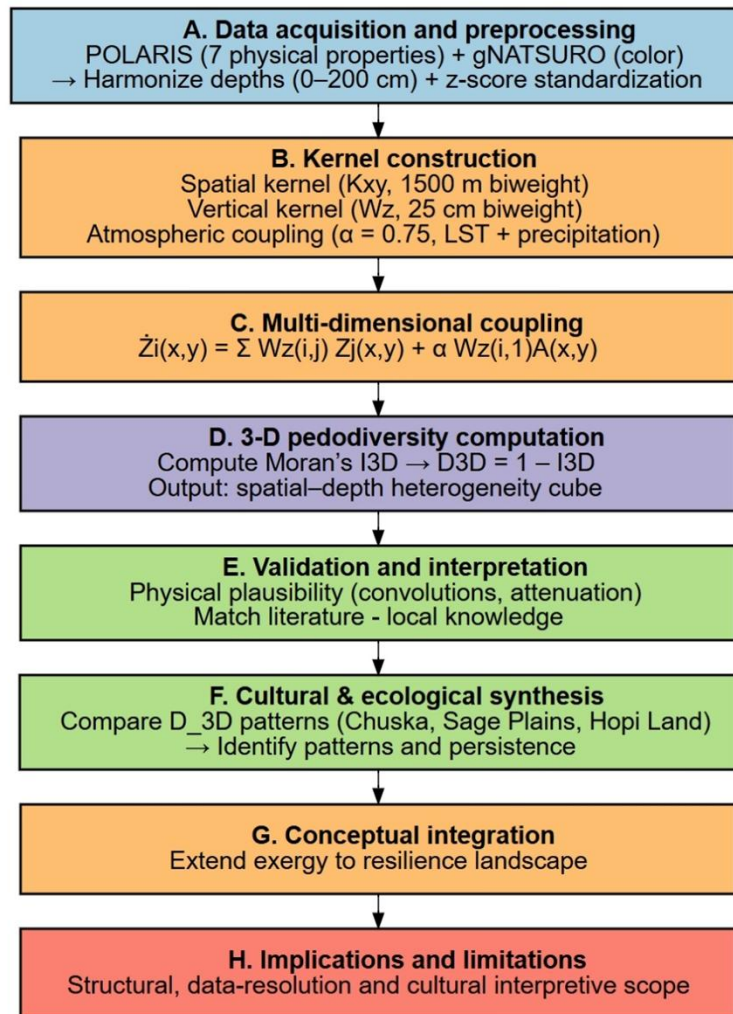
223 Since we are working with exergy states, we assume the reference state corresponds to a zero
224 gradient, representing no soil or the end of soil formation, the limits of a soil's life span.
225 Consequently, a zero gradient is assumed to indicate zero functionality and no resilience to
226 change, and the behavior determines which functions are expressed. Although this implicitly
227 implies linearity in time and ΔH , the model is not linear in these timers.

228 The σ function is fundamental for calculating pedocomplexity as defined here and the least
229 understood. Pedogenic states and pedodiversity represent two distinct and often conflicting
230 objective functions. While Ψ represents magnitude or a convergence process (e.g., the sum of
231 exergy across dimensions), σ represents arrangement or separation, which is a divergent process
232 (e.g., the covariance of exergy across dimensions). Although treating the problem as a voxel
233 increases the number of degrees of freedom relative to unknown parameters, the conflicting
234 objective functions exert a stronger influence and numerical stability drops significantly.

235 Perhaps most importantly, these conflicting objectives can create visualizations that appear
236 unrealistic despite mathematical stability, resulting in an effective function that is difficult to
237 interpret and limiting its accessibility. A concept highly emphasized in the framework is keeping
238 everything interpretable and easy to visualise. Consequently, we also want to create an index for σ
239 and thus, thermodynamic pedodiversity, which is σ scaled [0,1] or the process from [0,1]. Although
240 they are equivalent, it is important when mapping large regions depending on software or
241 environment used. Therefore, to solve $O(s)$, σ must be an energy-minimizing function that
242 increases (not decreases) across dimensions yet defines the spread and never falls below zero,
243 much like the spatial lag of variance.

244 2.3.2 Profile to landscape scale

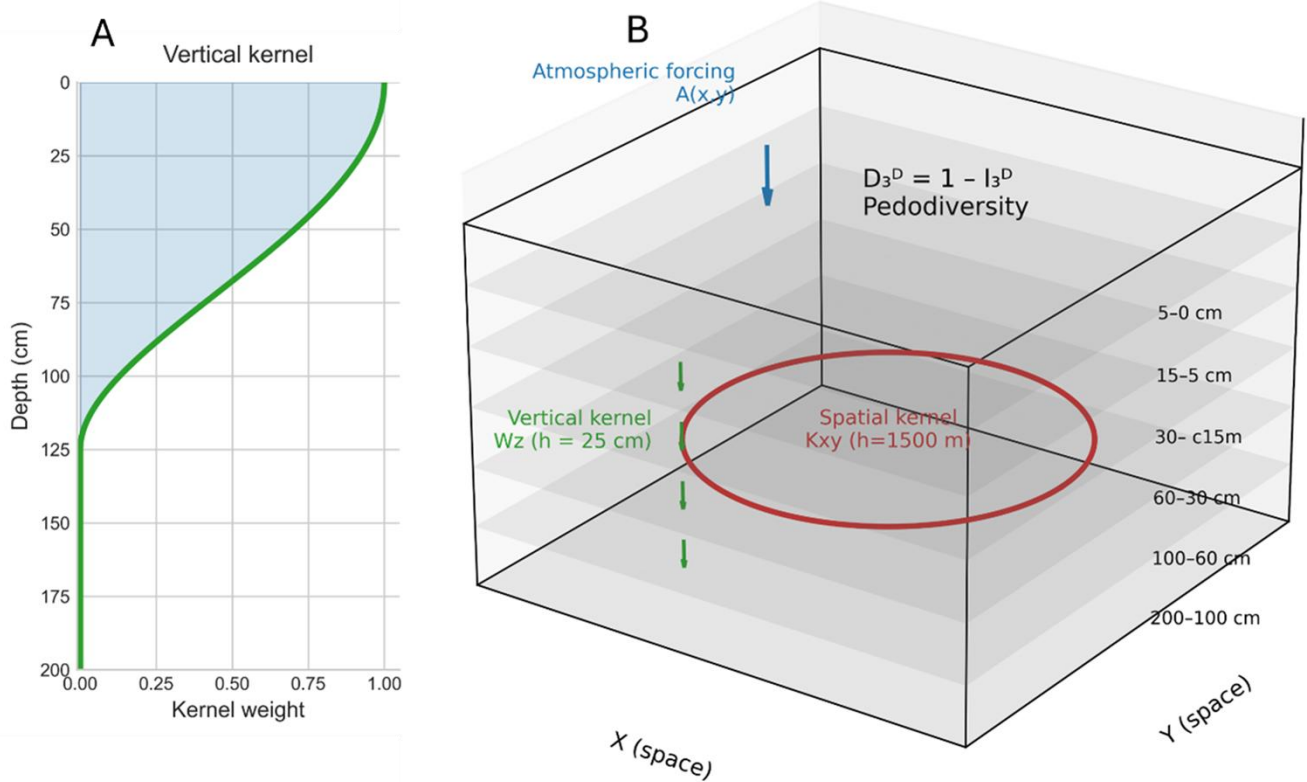
245 A mechanistic, multi-dimensional pedodiversity index was developed to represent the energy
246 transfer dynamics that regulate soil state dissipation energy. The index integrated eight gridded soil
247 properties across depth layers (image bands) using 3-dimensional biweight convolutions
248 constrained by physical continuity. This expresses pedodiversity as a coupled spatial–vertical
249 phenomenon, where spatial heterogeneity emerges from lateral and depth-dependent
250 interactions among soil properties (Ibáñez and Bockheim, 2013). Although not a direct measure of
251 soil functions, the index captures the organization and connectivity of exergy that is the foundation
252 to soil multifunctionality (Bünemann et al., 2018; Vogel et al., 2018). The process is straightforward
253 and can be represented schematically in linear form (Figure 2).



254

255 *Figure 2: flowchat of the incorporation of the thermodynamic pedodiversity into the larger synthesis of agroecosystem resilience.*

256 The complete pedodiversity computation, local mean and variance calculations and
 257 normalization of the three-dimensional Moran's I (Moran, 1950) was implemented entirely in the
 258 GEE Python API. This approach ensured computational scalability across all properties and
 259 depths, allowing the calculation of the pedodiversity directly from a spatially harmonized soil
 260 property cube (Figure 3). This represents a new methodological application of GEE, as it is rarely
 261 used for depth-dynamic or three-dimensional subsurface analyses, extending its capacity beyond
 262 traditional two-dimensional surface modeling.



263

264 *Figure 3: (A) Vertical curve generated from the biweights, illustrating depth-dependent coupling within the soil profile. (B) Spatial-*
 265 *vertical soil cube with atmospheric forcing $A(x, y)$. Together these components generate multidimensional coupling curves at each*
 266 *pixel, from which the pedodiversity index $D_{3D} = 1 - I_{3D}$ is calculated through the inverse of the three-dimensional Moran's I .*

267 2.3.3 Three-dimensional convolutions

268 Although the thermodynamic pedodiversity index was implemented as an integrated framework,
 269 the spatial and vertical convolutions were computed independently and then merged into one.
 270 This separation provided diagnostic insight into the relative weighting along each dimension,
 271 allowing the model to be fine-tuned toward physical realism and to extract validation information.
 272 The vertical component operates over millimeter- to centimeter-scales, whereas the spatial
 273 component extends over meter- to kilometer-scale gradients. The local horizontal and vertical
 274 interactions between pixels were modeled using a biweight convolution function defined as:

275
$$K_{xyz}(d) = \begin{cases} [1 - (d/h)^2]^2 & d > h \\ 0, & d < h \end{cases}$$

276 where d is the Euclidean distance in the vertical domain (K_z) and the spatial domain (K_{xy}), while h
277 is the bandwidth determining the maximum range of interaction. Both domains were subsequently
278 normalized so that their integrated weights summed to one. This gives an almost symmetrical
279 convolution, except where atmospheric forcing modified the weighting at the soil surface. The
280 weights were combined through matrix algebra when implementing the algorithm. The biweighting
281 was used because it provides a smooth, finite-support weighting function that emphasizes local
282 interactions (Beaton and Tukey, 1974; Hengl et al., 2004), while preventing long-distance artifacts
283 (Press, 2007).

284 2.3.4 Atmospheric boundary

285 Many soil depth functions have considered how to handle boundary conditions of the profile.
286 While an exact analytical spline will solve this boundary problem, additional functions can be used
287 if atmospheric forcing is applied, soil profile exergy never becomes zero gradient and may have
288 implications for things like numerical classification pedocomplexity.

289 Since the topsoil forms the physical boundary of many atmospheric–pedologic interactions (e.g.,
290 infiltration, evaporation and heat exchange), an atmospheric forcing term $A(x, y)$ was introduced
291 as a boundary condition:

293
$$\tilde{Z}_i(x, y) = \sum_{j=1}^n W_z(i, j) Z_j(x, y) + \alpha W_z(i, 1) A(x, y)$$

292

294 where $Z_j = X_j - \bar{X}$ represents deviations of soil property X_j from its mean, α is the coupling
295 coefficient controlling the magnitude of atmospheric influence and $W_z(i, 1)$ diffusion through the
296 surface to lower depths. This formulation is like the Robin boundary condition (Gustafson and Abe,
297 1998), which combines flux and state terms to represent the exchange of energy or mass across
298 boundaries. Here, it allows surface energy and moisture fluxes to be transported, stored and
299 transformed through the soil profile, linking atmospheric variability directly to sub-surface
300 processes.

301 2.3.5 Objective function

302 The objective function used in this study equates to the inverse 3-dimensional Moran's I. Which is
303 the process that scales to [0,1] and can be used as an index and the pedogenic exchange loss
304 function in pedocomplexity. However, it needs to be accumulating at each pixel and energy
305 minimizing. Additionally, the function must calculate spatial heterogeneity where it essentially
306 collapses back into an energy form. This effectively makes it consistent in the framework, the
307 spatial lag of variance represents pedodiversity and increases computation as the function
308 simplifies.

309 For the objective function, we need the interaction energy density where local interactions
310 accumulate:

$$311 \quad E = \frac{1}{V} \sum_{i,j} J_{ij} s_i s_j$$

312 Where s is the variable state, J_{ij} is the coupling strength between the two states normalized by the
313 volume. When defining the local Moran's I for the 3-dimensional convolution (I_3) and reframing it
314 for energy dissipation, we get thr equation:

315
$$\sigma(x, y) = 1 - (I_3) = 1 - \frac{\sum_{i=1}^n \tilde{Z}_i(x, y) \tilde{Z}_{i,local}(x, y)}{n \cdot Var(X)(x, y)}$$

316 Here, $\tilde{Z}_{i,local}$ represents the horizontal mean of the standardized property, \tilde{Z}_i using the spatial
317 weights and $Var(X)$ denotes the local variance computed across depths (n) within the vertical
318 weights.

319 Related to the interaction energy density, the $\tilde{Z}_{i,local}$ interacting state, the \tilde{Z}_i the state variable and
320 normalized by $n \cdot Var(X)$. As we are calculating the from the data over the dimensions, summation
321 calculates the strength of coupling. Most importantly, it collapses back to a Dirichlet energy when
322 summed across space.

323
$$E = \int |\nabla Z|^2 dx$$

324 Thus, fitting the requirements for the thermodynamic pedodiversity objective function within the
325 broader context of pedocomplexity.

326 The pedocomplexity objective function would ideally be linear solvable. However, the inverse
327 Moran's I equation is deterministic and computationally efficient. Therefore, it could be used as an
328 interpretable index and used in a more complex function to solve pedocomplexity, thus lowering
329 the computational cost for large areas. This makes it ideal for both an index and for later
330 computation as it solves the process and is visually interpretable without manipulation.

331 2.3.6 Implementation

332 The framework was implemented in GEE to ensure computational scalability across large spatial
333 extents. The pedodiversity index was computed using a soil property image cube harmonized to
334 six standard depths. The soil properties were all converted to global z-scores per depth, where the

335 mean equals 0 and standard deviation equals 1. Global z-scores were used to ensure each
336 property contributes equally, scale invariant and to ensure physical meaning.

337 The horizontal domain had a maximum range of $h_m = 1,500$ m with a radius of 7 pixels and a spatial
338 scale of 30 m, representing lateral field-to-field influence distances. The vertical domain used
339 $h_z = 25$ cm as the effective correlation length between soil horizons, consistent with observed
340 horizon thicknesses and infiltration depths. Atmospheric coupling ($\alpha = 0.75$) was applied only to
341 the surface horizon to simulate boundary energy fluxes driven by surface temperature or
342 precipitation and releasing exergy. Land surface temperature was obtained from cloud-masked
343 Landsat 8 and 9 (USGS, 2021) imagery using the median composite for 2024, while precipitation
344 data were obtained from NASA's Global Precipitation Measurement (GPM) mission, specifically
345 the Integrated Multi-satellite Retrievals for GPM (IMERG) product (Huffman et al., 2023), by
346 summing the total precipitation for the year 2024.

347 2.4 Validation and evaluation

348 Both quantitative and qualitative analyses were conducted on the multi-dimensional
349 pedodiversity index. Quantitatively, we evaluated how the vertical, spatial and atmospheric
350 coupling components behaved in physically plausible ways and how much of the observed
351 variation was explained by intrinsic soil properties. Qualitatively, we examined whether the
352 patterns identified by the index aligned with documented traditional practices, drawing on local
353 dryland farming literature, anthropological studies and Indigenous ecological knowledge of the
354 region. Integrating these perspectives was essential to interpret the pedodiversity patterns within
355 their cultural and environmental context and without such knowledge, our understanding of the

356 past and present soil conditions remains incomplete, and our ability to adapt to future climate
357 change is fundamentally limited (Whyte, 2013).

358 3 Results and discussion

359 We developed a thermodynamic pedodiversity index that integrates eight soil properties along with
360 their depth continuity through a 3-dimensional convolution to quantify soil state pedodiversity
361 across multiple scales. This approach treats pedodiversity as an energy-density distribution,
362 capturing how exergy gradients are arranged and dispersed throughout physical space. By moving
363 beyond layer-based or taxonomic frameworks, this multidimensional method provides a
364 mechanistic representation of soil structure, offering a foundational perspective on soil systems
365 and the management decisions shaping diverse agroecosystems in the U.S. Southwest.

366 3.1 Vertical and spatial structure

367 The convolutions revealed a strongly stratified pattern of soil energy exchange. The upper 5–30 cm
368 formed the dominant zone of vertical coupling (Table 2), acting as an interface where atmospheric
369 interactions, anthropotropic activity, organic matter inputs and bioturbation generate high spatial
370 heterogeneity. Below ~60 cm, the strongly decoupled state reflects a shift toward a
371 thermodynamic and structural steady state, where minimal energy exchange preserves inherited
372 contrasts in texture and compaction, and biological contributions to surface-driven ecosystem
373 functions are greatly reduced (Wang, 2010). These deeper layers exert long-term influence on
374 rooting depth and drought buffering but play a smaller role in short-term cultivation dynamics.

375 *Table 2: Vertical weight bisquared matrix from purely soil properties*

	0-5 cm	5-15 cm	15-30 cm	30-60 cm	60-100 cm	100-200 cm
--	--------	---------	----------	----------	-----------	------------

0-5 cm	0.511	0.423	0.066	0	0	0
5-15 cm	0.436	0.418	0.235	0	0	0
15-30 cm	0.075	0.325	0.579	0.021	0	0
30-60 cm	0	0	0.035	0.965	0	0
60-100 cm	0	0	0	0	1	0
100-200 cm	0	0	0	0	0	1

376

377 When atmospheric forcing was incorporated through land-surface temperature and precipitation
378 coupling at the surface boundary, the convolution emphasized the 5–15 cm horizon as the primary
379 energy mediator rather than the boundary 0-5 cm layer (Table 3). This suggests that the topsoil acts
380 as a rapid transient layer, whereas the subsurface horizon functions as the primary buffer, storing
381 and redistributing moisture and heat with delayed release acting as a stabilizing feature in drought-
382 prone agricultural systems. Nevertheless, the 0–5 cm layer can shift to a primary energy-input zone
383 for water and nutrients during germination, illustrating how soil multifunctionality emerges
384 dynamically in response to plant establishment in dryland systems.

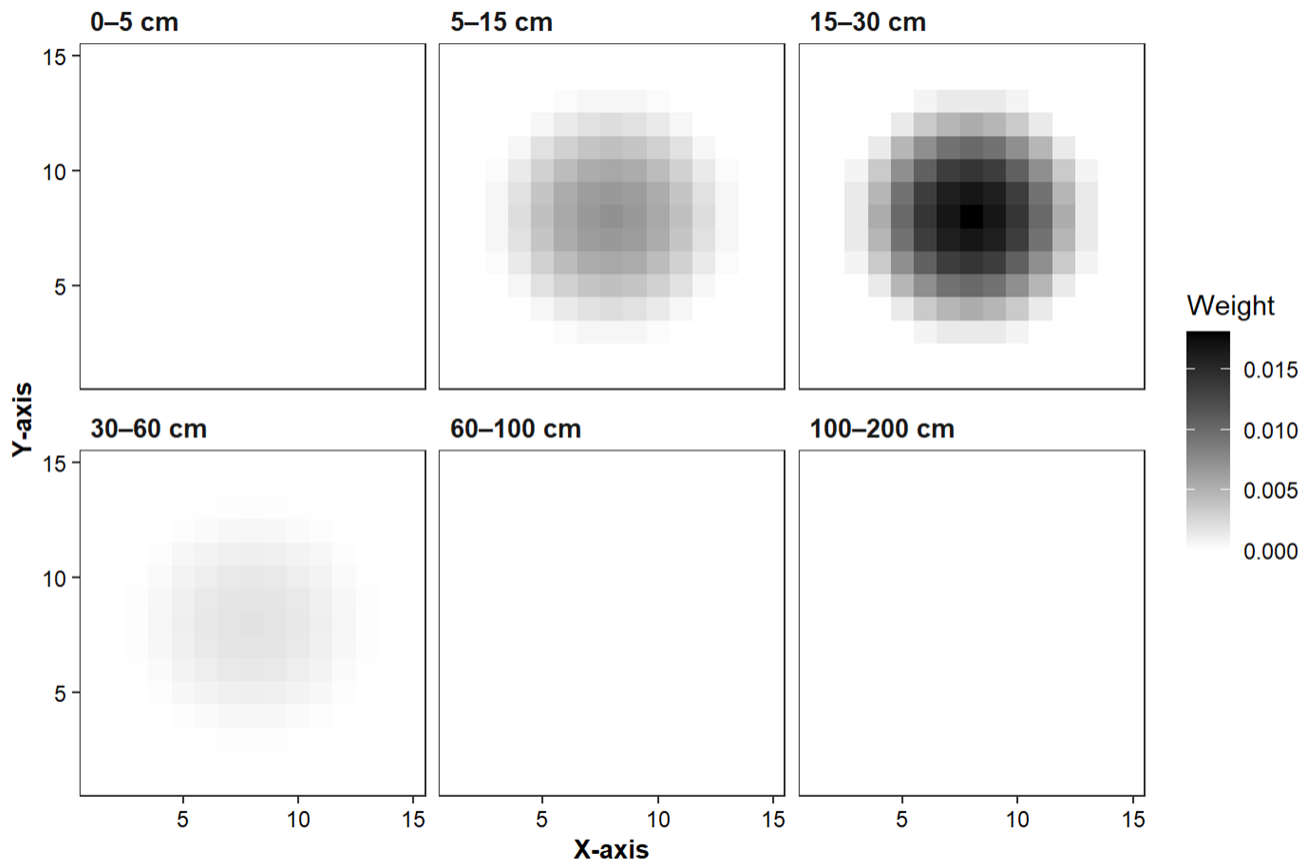
385 *Table 3: The combined vertical weights incorporating influences from the atmosphere and the soil.*

	0-5 cm	5-15 cm	15-30 cm	30-60 cm	60-100 cm	100-200 cm
0-5 cm	0.239	0.658	0.103	0	0	0
5-15 cm	0.137	0.552	0.311	0	0	0
15-30 cm	0.024	0.344	0.611	0.022	0	0
30-60 cm	0	0	0.035	0.965	0	0
60-100 cm	0	0	0	0	1.000	0
100-200 cm	0	0	0	0	0	1.000

386

387 Spatial convolution patterns further reinforced this structure (Figure 4): high surface connectivity,
388 peak process diversity at intermediate depths and reduction toward deeper horizons. Functionally,
389 this identifies the zone of maximum agricultural responsiveness, the horizons most critical for crop
390 establishment, root exploration and moisture capture in arid environments. It should be noted that

391 the convolution weights represent the relative intensity of vertical and lateral energy exchange;
392 however, a single convolution configuration was applied uniformly across all sites.



393

394 *Figure 4: spatial and vertical interactions, note that there is a kernel applied through all depths, and this shows where the energy*
395 *appears to be interacting.*

396 The observed differences among depth layers arise from the soil property distributions themselves
397 rather than from learned or adaptive convolution weights as used in deep learning or neural
398 network architectures. In this framework, the convolution acts as a physics-informed coupler, not
399 a data-trained filter, allowing soil heterogeneity relevant to exergy potential to emerge directly from
400 the underlying soil matrix. Figure 4 illustrates the base convolution form and how its interactions
401 reveal shifts in soil characteristics to soil processes across the landscape.

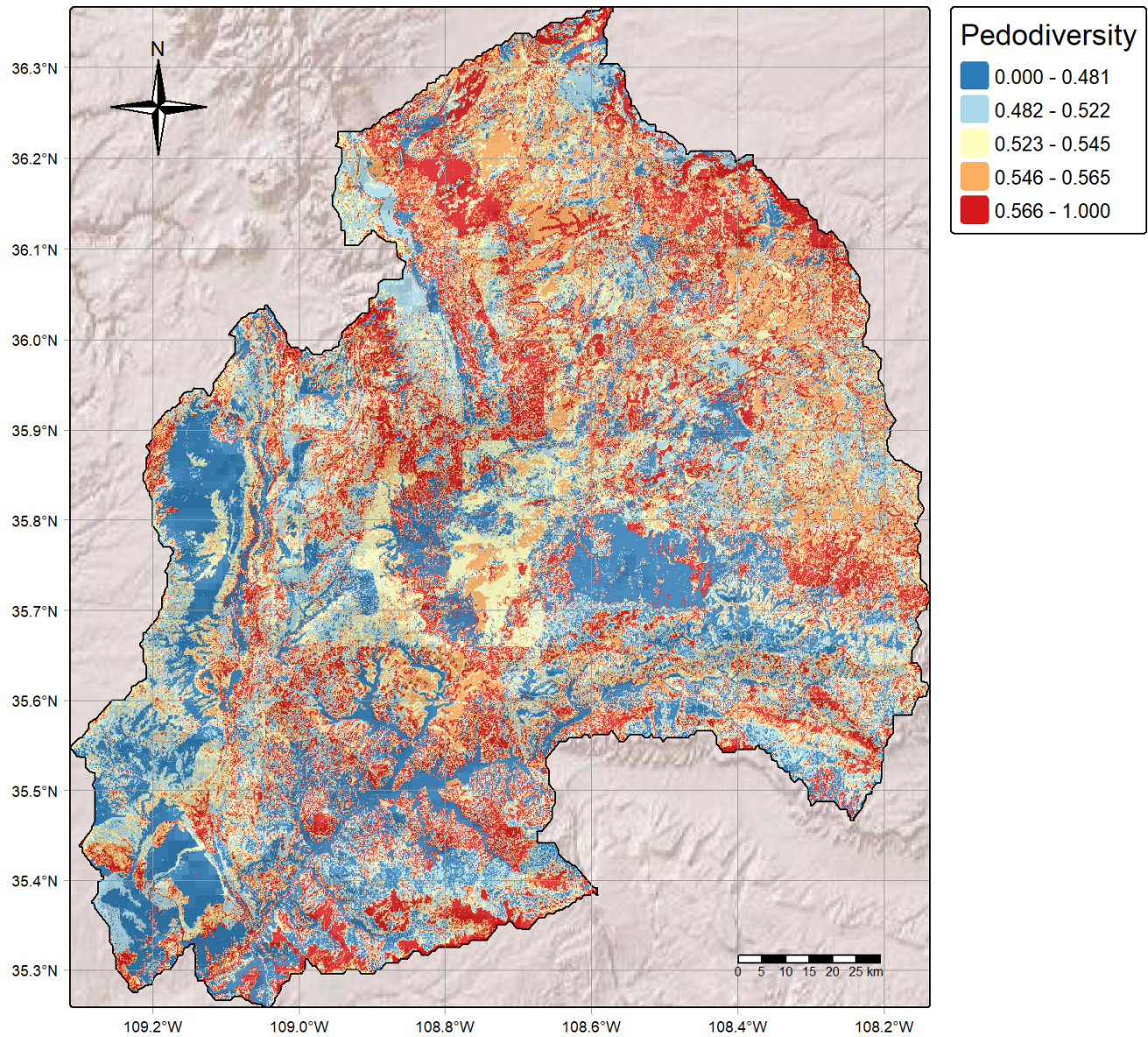
402 3.2 Spatial interpretation

403 The pedodiversity index align closely with areas historically associated with Ancestral Pueblo
404 agriculture and long-term resilient farming traditions, reinforcing the connection between soil
405 organization and adaptive land management (Pawluk, 1995). However, when interpreting a
406 second-order voxel diversity index, it is important to recognize that higher values represent greater
407 diversity in soil exergy states and composition, not necessarily more favorable conditions for a
408 specific function or crop. Therefore, ground truth is needed to evaluate this functionality. In this
409 context, pedodiversity reflects the potential for resilient outcomes rather than a direct measure of
410 fertility or productivity (Handayani and Prawito, 2010). In other words, it represents the variety of
411 choices present at a given location.

412 3.2.1 Chuska Mountains

413 The southern Chuska Mountains, the southern basin and its piedmont (Figure 5) span lands long
414 inhabited by the Navajo peoples, where the soil and landforms have shaped, and been shaped by,
415 diverse land use traditions (Pawluk, 1995). Along the northeastern slopes and piedmonts, soil of
416 high pedodiversity (>0.50) developed where volcanic and sandstone parent materials merge
417 through colluvial–alluvial processes across steep topographic gradients (Reneau et al., 1996;
418 Seager et al., 1987). This heterogeneity, combined with contrasting moisture and temperature
419 regimes, created many ecological niches from the timbered ridges to the cultivated footslopes
420 once supporting maize, bean and squash gardens connected to the Chaco Canyon network
421 (Doolittle, 2000; Vivian and Hilpert, 2012). At higher elevations, timber resources rather than

422 agriculture dominated, with the diversity of soil reflecting climate and forest–soil interactions more
423 than intensive land management (Allen et al., 1998; Huckell, 1996).



424

425 *Figure 5: spatial thermodynamic pedodiversity index of the southern Chuska Mountains and southern basin.*

426 Southward, the Chuska Basin transitions to a low-pedodiversity landscape (<0.50) where aeolian
427 sands, episodic rainfall and the shadow of the northern volcanic crest constrain soil development
428 and vegetation complexity (McFadden et al., 1998; Seager et al., 1987). Within this more uniform

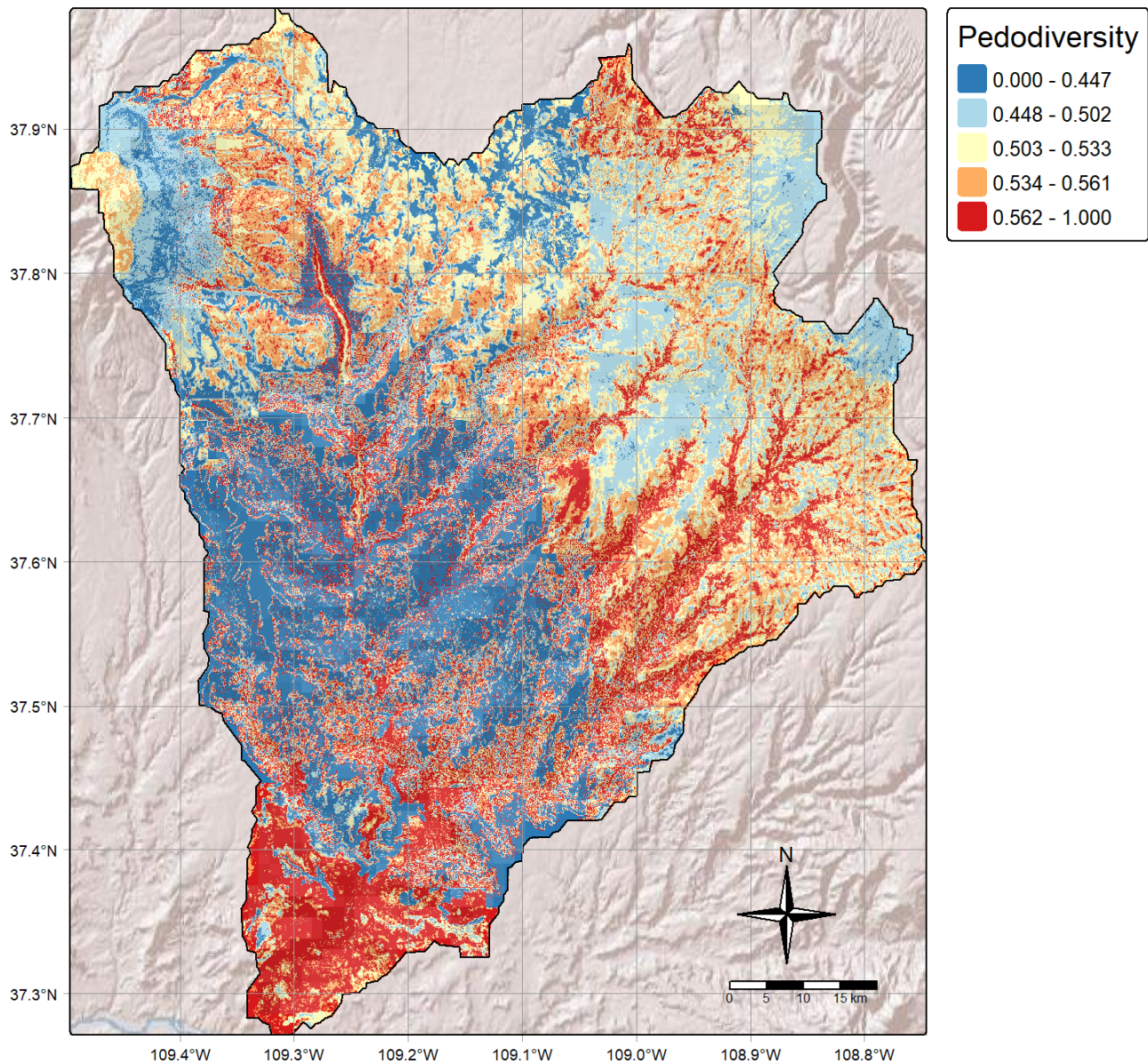
429 terrain, the Navajo pastoral tradition remains sustainable; an ecological adaptation emphasizing
430 mobility, grazing flexibility and stewardship of scarce resources (Redsteer et al., 2018; Weisiger,
431 2004). The pedodiversity contrast between the mountain flanks and the basin floor thus parallels
432 the entangled relationships of geomorphology, soil formation and cultural adaptation across this
433 sacred and resource-rich landscape (Doolittle, 2000; Pawluk, 1995).

434 Importantly, this pattern also reflects how differences in soil multifunctionality shaped land-use
435 strategies: high-pedodiversity zones supported diverse cultivation niches, whereas low-
436 pedodiversity soil favored pastoral systems better suited to limited resource options. However, the
437 Chuska landscape exhibits a high degree of patchiness (Gini coefficient = 0.71). Although the
438 reasons for the reorganization of Chaco Canyon around 1100 A.D. remain debated, the
439 unpredictability of these soil niches would likely have made crop production difficult to sustain
440 during periods of environmental stress.

441 3.2.2 Great Sage Plain

442 The uplands surrounding the Great Sage Plains, north of Mesa Verde, exhibited moderate
443 pedodiversity values (≈ 0.48 – 0.54) across broad loess-covered plains and low-relief valleys (Figure
444 6). Unlike the deeply incised mesas to the south (Mesa Verde), this landscape consists primarily
445 of Mancos Shale–derived soil mantled by wind-blown silt and fine alluvium, producing gently
446 layered profiles with limited textural contrast (Harden and Taylor, 1983). These conditions favored
447 large, relatively homogeneous fields capable of retaining moisture from seasonal snowmelt,
448 supporting the extensive dryland agriculture practiced by Ancestral Pueblo communities during
449 the later Mesa Verde period (Kohler et al., 2008). Pockets of higher pedodiversity appear along
450 drainage heads and valley margins, where shallow colluvium and slope wash over shale enhanced

451 local water storage and nutrient heterogeneity. Such microenvironments likely provided greater
452 cropping stability during drought cycles, helping to sustain maize-based agriculture at the
453 northernmost frontier of Ancestral Pueblo settlement (Benson et al., 2007; Ortman, 2016).



454

455 *Figure 6: spatial thermodynamic pedodiversity index of the Great Sage Plains on the Colorado and Utah border.*

456 Compared with the high-pedodiversity of the Chuska uplands, where ash-rich parent materials
457 created abundant moisture niches, the Great Sage Plains strength lay in its spatial continuity and

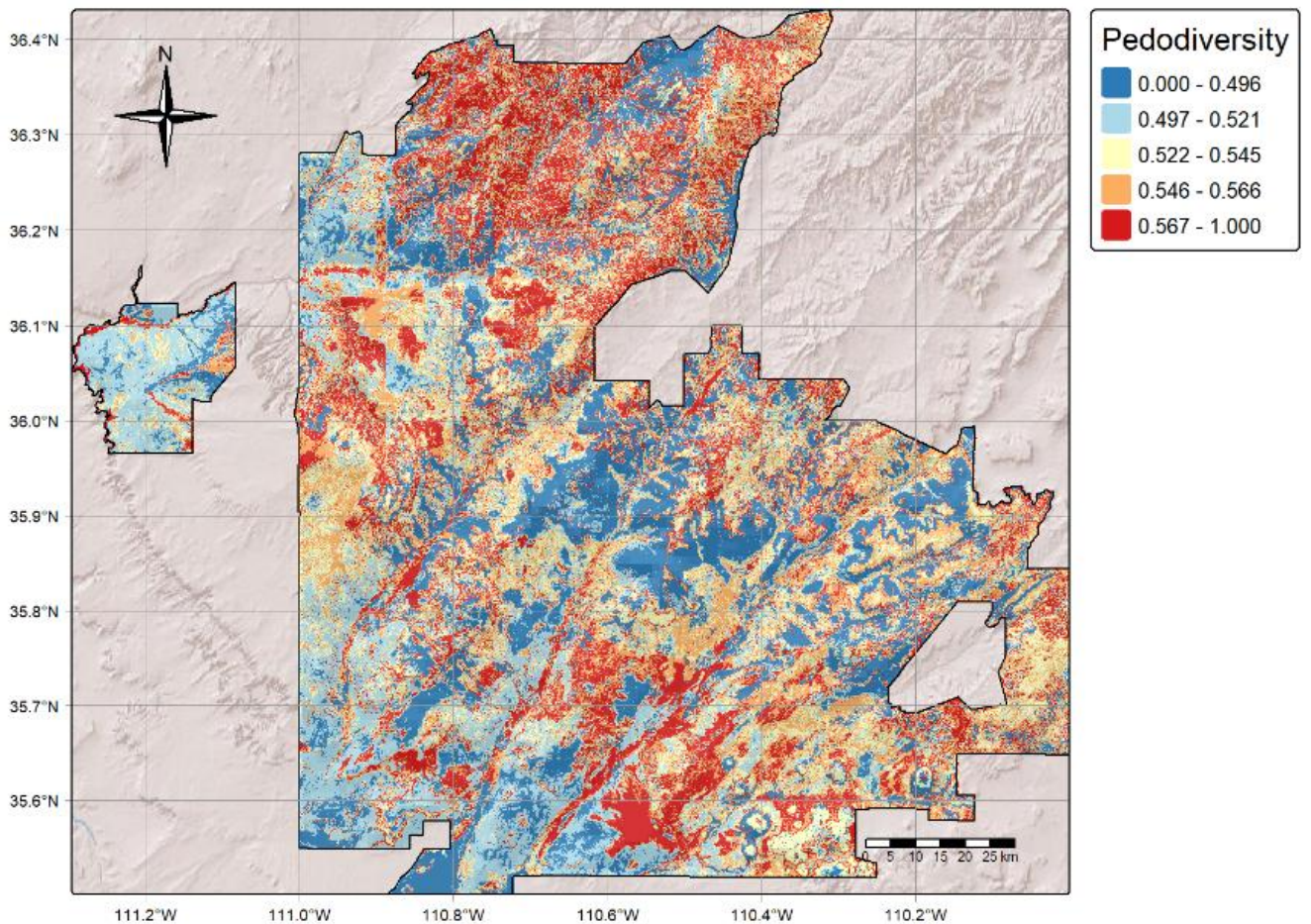
458 moisture buffering of uniform silty soil, enabling scale and labor efficiency rather than fine-
459 resolution niche exploitation for cultivation (Harden and Taylor, 1983). It represents a functionally
460 productive but less complex agricultural system; however, one more vulnerable to multi-year
461 drought and shortened growing seasons (Benson, 2011). Additionally, the absence of spatial
462 patterns in areas typically assumed to be agricultural land (e.g., fertile valley bottoms) would make
463 soil niches difficult to utilize. The pedodiversity pattern thus helps explain both the intensity of late
464 Ancestral Pueblo farming on the Great Sage Plain (Bocinsky and Kohler, 2014) and the sensitivity
465 of this northern margin to climatic downturns that contributed to regional reorganization in the late
466 13th century (Benson et al., 2007; Kohler et al., 2008).

467 3.2.3 Hopi Land

468 The Hopi Mesas and surrounding uplands exhibit moderate to high pedodiversity values (≈ 0.52 –
469 0.56), concentrated along mesa margins, valley breaks and colluvial footslopes (Figure 7). These
470 areas reflect sandstone and shale parent materials, colluvial reworking and fine-scale topographic
471 variation that together created a variety of soil textures and drainage conditions (Hack, 1942). Such
472 heterogeneity has historically supported the remarkable agricultural and biological diversity of the
473 Hopi landscape, one of North America's longest-inhabited dryland farming regions (Adler, 1996;
474 Cameron, 1999; Whiteley, 2008).

475 The Hopi cultivate drought-tolerant blue, red and white corns alongside beans, squash, melons
476 and medicinal herbs each adapted to subtle differences in soil conditions (Ferguson and Colwell-
477 Chanthaphonh, 2006; Sekaquaptewa and Washburn, 2004). Areas of elevated pedodiversity
478 correspond closely with traditional field systems where microtopographic and textural diversity
479 enhance soil–water–plant interactions, buffering crops against drought and temperature extremes

480 (Berkes, 2017). These pedodiversity-rich zones form part of a broader biocultural hotspot, where
481 long-term human stewardship and soil variability together sustain both agro-biodiversity and
482 ecosystem resilience across centuries of arid-land cultivation (Kimmerer, 2013; Müller and
483 Munroe, 2014; Muller et al., 2017).



484

485 *Figure 7: spatial thermodynamic pedodiversity index of the Hopi Land, Arizona.*

486 Across the regions, Hopi Land represent an intermediate position between the high-contrast
487 landscape of the Chuska Mountains and the more homogeneous loessal surface of the Great Sage
488 Plains. However, unlike the steep and climatically stratified Chuska slopes, Hopi soil occurred
489 within a more stable, low-relief plateau environment, where subtle heterogeneity rather than

490 abrupt contrasts determined the thermodynamic diversity (Hendricks, 1985). It is thought that this
491 caused a relatively more ordered pedodiversity, with clear patterns. The result was a balanced soil
492 structure that sustains both resilience and crop productivity under arid conditions, with
493 knowledge or identifiers of these patterns (Bousselot et al., 2017).

494 In contrast to the Sage Plain's broad, uniform agricultural surfaces, Hopi fields are intentionally
495 distributed across exergy states ranging from sandy, fast-draining uplands to heavier alluvial
496 footslopes, creating a variety of soil microenvironments that support exceptional agro-biodiversity
497 (Cleveland et al., 1994; Rea, 1997). This adaptability, rooted in the Hopi's knowledge of soil and
498 topographic variation, mirrors the broader pattern observed across the Southwest: an
499 understanding of soil niches and the soil system is often more critical for maintaining a resilient
500 agroecosystem than the absolute level of pedodiversity or whether a culture relies on a crop-
501 dominant or pastoral system (Armstrong et al., 2021; Redsteer et al., 2018). Consequently,
502 pedodiversity is thought to support only a portion of soil multifunctionality, largely independent of
503 cultural factors, though concepts such as pedocomplexity may offer a more integrated
504 perspective.

505 3.3 Implications and limitations

506 The framework provides a quantitative bridge between pedodiversity, ecosystem services and
507 food-system resilience. By representing soil as a coupled continuum, the approach identified
508 zones of intrinsic interactions that may serve as biophysical indicators for resilient agriculture and
509 climate adaptation planning with the help of continuous indigenous knowledge (Bünemann et al.,
510 2018; Dominati et al., 2010). The explicit physical formulation also enables integration with a
511 broad range of scientific disciplines from physics to economics, providing a scalable tool for

512 extrapolating resilience potential in contemporary agroecosystems facing intensifying climatic
513 stress. At the fundamental level, it shows the diversity of soil and highlights benefits and possible
514 misconceptions of pedodiversity. However, it is a second-order multidimensional continuous form
515 of the index, which may be difficult to interpret.

516 This study revealed that the spatial pattern of pedodiversity is just as important as pedodiversity
517 itself. Although thermodynamic pedodiversity incorporates multiple dimensions and represents a
518 second-order pedodiversity index, societies with long histories of resilient agriculture appear to
519 have made land-use decisions based on higher-order states beyond pedodiversity alone,
520 consistent with the concept of pedocomplexity. This realization is important both mathematically
521 and philosophically for resilience research. While current approaches move in the right direction,
522 they remain incomplete and require a more rigorous foundation. Integrating mathematical
523 frameworks with Indigenous ecological knowledge will be essential for advancing our
524 understanding of agroecosystem resilience.

525 Therefore, several limitations should be acknowledged. First, this study assumes that societies
526 made land-use decisions primarily to maintain agroecosystem resilience and soil
527 multifunctionality, given the semi-arid, drought-prone environment that necessitates careful
528 management of water, crops, and soils. Sites such as Hopi lands, with continuous cultivation over
529 millennia, or regions with significant Ancestral Pueblo population growth, were selected in part to
530 justify these assumptions. However, this framework does not account for other influencing
531 factors, including agricultural diseases, cultural practices unrelated to agriculture, internal
532 political pressures, geographic constraints, external conflicts and numerous other socio-
533 environmental constraints. While site selection was intended to minimize these confounding
534 influences, it cannot be assumed that all pressures were independent or concurrent. Further

535 research is needed to incorporate these additional dimensions into the pedocomplexity
536 framework.

537 The framework identifies pedodiversity that may correlate with historical land use, but it does not
538 claim to reconstruct the full decision-making, symbolic or social dimensions of Ancestral Pueblo,
539 Navajo or Hopi agricultural systems (Handayani and Prawito, 2010; Kimmerer, 2013). Pedodiversity
540 patterns provide biophysical context, not direct evidence of cultural intent. Moreover, ancestral
541 land use strategies were guided by complex ecological knowledge, spiritual values and
542 multigenerational adaptation that cannot be fully represented by soil processes alone (Berkes,
543 2017; Reo and Whyte, 2012). Interpretations of past agroecosystems should therefore
544 complement, not replace, Indigenous knowledge.

545 The framework measures thermodynamic diversity rather than explicit biological, chemical or
546 agronomic functionality; thus, high pedodiversity does not necessarily equate to high fertility or
547 crop productivity (Nielsen and Wendroth, 2003). Extensive evaluation is required to correlate it
548 with soil morphological, crop yield, function and laboratory analyses in order to realize the full
549 potential of thermodynamic pedodiversity and, ultimately, pedocomplexity. At a fundamental
550 level, it can help explain aspects of soil multifunctionality together with exergy states and latent
551 energy; however, evaluating these innovations requires a comparable level of effort.

552 The use of gridded national soil property datasets (e.g., POLARIS, gNATSURO) introduces
553 uncertainties associated with interpolation and coarse resolution, which may obscure fine-scale
554 heterogeneity that is critical for farm-level decision-making (Chaney et al., 2016). Third, while the
555 biweight convolution provides a realistic finite-support coupling, it assumes isotropic distribution
556 and may underestimate anisotropic behaviors such as preferential flow, layered permeability or

557 root-mediated transport (Bear, 1972; Jury and Horton, 2004) , all of which can strongly influence
558 agroecosystems.

559 By quantifying pedodiversity directly through the 3-dimensional Moran's I, we establish a spatially
560 explicit foundation that integrates seamlessly with our broader framework for assessing soil
561 resilience and multifunctionality, providing a mechanistic basis for interpreting how soil structure
562 and management practices interact across heterogeneous Indigenous dryland agroecosystems.
563 Future work should develop a formal mathematical formulation of pedocomplexity and investigate
564 how these thermodynamic states correspond to morphological features on indigenous lands that
565 support resilient agroecosystems.

566 4 Conclusion

567 Understanding pedodiversity through a mechanistic, multidimensional framework provides a
568 powerful means of linking soil thermodynamics to landscape scale patterns that support food
569 production and long-term agroecosystem resilience. By quantifying the spatial-vertical variation
570 and rare states of soil processes, this approach identifies zones of high multivariate variability,
571 where thermodynamics broadens the range of soil niche identification. At the same time, it
572 clarifies how societies have historically adapted to these gradients: from the mobile, drought-
573 responsive pastoral systems of the Navajo to the selective crop breeding and field placement
574 strategies of the Hopi that have sustained dryland agriculture for millennia, to the agricultural
575 intensification on more homogeneous soil that may have contributed to the abrupt reorganization
576 of the Mesa Verde Ancestral Pueblo. Most importantly, pedodiversity demonstrates that it is not
577 diversity per se that drives land-use decisions, but the spatial patterns of pedodiversity reflecting

578 higher-order processes that govern soil resilience and multifunctionality (i.e., pedocomplexity).
579 Modern agricultural and conservation strategies can benefit from recognizing that these soil
580 heterogeneity patterns form the biophysical foundation of productive, resilient food systems, just
581 as they have for Indigenous agroecosystems in the U.S. Southwest. In this way, pedodiversity
582 highlights soil not merely as a substrate for crop production, but as a dynamic archive of human–
583 environment interactions, offering guidance for sustainable farming into the future.

584 References

- 585 Adler, M., 1996. *The Prehistoric Pueblo World, A.D. 1150-1350*. University of Arizona Press.
- 586 Allen, C., Betancourt, J., Swetnam, T., 1998. Landscape changes in the southwestern United
587 States: Techniques, long-term datasets, and trends, in: *Perspectives on the Land Use*
588 *History of North America*, Biological Science Report. U.S. Geological Survey, Lafayette, LA,
589 pp. 71–84.
- 590 Allison, J., 2010. The End of Farming in the “Northern Periphery” of the Southwest, in: *Leaving Mesa*
591 *Verde: Peril and Change in the Thirteenth-Century Southwest*. University of Arizona Press,
592 Tuscon.
- 593 Appledorn, C.R., Wright, H.E., 1957. VOLCANIC STRUCTURES IN THE CHUSKA MOUNTAINS,
594 NAVAJO RESERVATION, ARIZONA–NEW MEXICO. *Geol Soc America Bull* 68, 445.
595 [https://doi.org/10.1130/0016-7606\(1957\)68%255B445:VSITCM%255D2.0.CO;2](https://doi.org/10.1130/0016-7606(1957)68%255B445:VSITCM%255D2.0.CO;2)
- 596 Armstrong, C.G., Miller, J.E.D., McAlvay, A.C., Ritchie, P.M., Lepofsky, D., 2021. Historical
597 Indigenous Land-Use Explains Plant Functional Trait Diversity. *E&S* 26, art6.
598 <https://doi.org/10.5751/ES-12322-260206>
- 599 Arrouays, D., McKenzie, N., Hempel, J., Richer de Forges, A., McBratney, A., 2014. GlobalSoilMap:
600 Basis of the global spatial soil information system, in: Arrouays, D., McKenzie, N., Hempel,
601 J., Richer de Forges, A., McBratney, A.B. (Eds.), . Presented at the 1st GlobalSoilMap
602 Conference, CRC Press, Orleans, France.
- 603 Bagley, J.E., Davis, S.C., Georgescu, M., Hussain, M.Z., Miller, J., Nesbitt, S.W., VanLoocke, A.,
604 Bernacchi, C.J., 2014. The biophysical link between climate, water, and vegetation in
605 bioenergy agro-ecosystems. *Biomass and Bioenergy* 71, 187–201.
606 <https://doi.org/10.1016/j.biombioe.2014.10.007>
- 607 Bear, J., 1972. Dynamics of Fluids in a Porous Media. *J. Fluid Mech.* 61, 206–208.
608 <https://doi.org/10.1017/S0022112073210662>
- 609 Beaton, A.E., Tukey, J.W., 1974. The Fitting of Power Series, Meaning Polynomials, Illustrated on
610 Band-Spectroscopic Data. *Technometrics* 16, 147–185.
611 <https://doi.org/10.1080/00401706.1974.10489171>

612 Bellorado, B.A., Anderson, K.C., 2013. EARLY PUEBLO RESPONSES TO CLIMATE VARIABILITY:
613 FARMING TRADITIONS, LAND TENURE, AND SOCIAL POWER IN THE EASTERN MESA
614 VERDE REGION. *KIVA* 78, 377–416. <https://doi.org/10.1179/0023194013Z.0000000007>

615 Benson, L., 2011. Factors Controlling Pre-Columbian and Early Historic Maize Productivity in the
616 American Southwest, Part 1: The Southern Colorado Plateau and Rio Grande Regions. *J*
617 *Archaeol Method Theory* 18, 1–60. <https://doi.org/10.1007/s10816-010-9082-z>

618 Benson, L., Cordell, L., Vincent, K., Taylor, H., Stein, J., Farmer, G.L., Futa, K., 2003. Ancient maize
619 from Chacoan great houses: Where was it grown? *Proc. Natl. Acad. Sci. U.S.A.* 100, 13111–
620 13115. <https://doi.org/10.1073/pnas.2135068100>

621 Benson, L., Petersen, K., Stein, J., 2007. Anasazi (Pre-Columbian Native-American) Migrations
622 During The Middle-12Th and Late-13th Centuries – Were they Drought Induced? *Climatic*
623 *Change* 83, 187–213. <https://doi.org/10.1007/s10584-006-9065-y>

624 Berkes, F., 2017. *Sacred Ecology*, 4th ed. Routledge. <https://doi.org/10.4324/9781315114644>

625 Blagbrough, J.W., 1967. Cenozoic geology of the Chuska Mountains, in: *Defiance-Zuni-Mt. Taylor*
626 *Region, Arizona and New Mexico*. Presented at the 18th Annual Fall Field Conference, New
627 Mexico Geological Society, pp. 70–77. <https://doi.org/10.56577/FFC-18.70>

628 Bocinsky, R.K., Kohler, T.A., 2014. A 2,000-year reconstruction of the rain-fed maize agricultural
629 niche in the US Southwest. *Nat Commun* 5, 5618. <https://doi.org/10.1038/ncomms6618>

630 Bocinsky, R.K., Varien, M.D., 2017. Comparing Maize Paleoproduction Models with Experimental
631 Data. *Journal of Ethnobiology* 37, 282–307. <https://doi.org/10.2993/0278-0771-37.2.282>

632 Bousset, J., Muenchrath, D., Knapp, A., Reeder, J., 2017. Emergence and Seedling
633 Characteristics of Maize Native to the Southwestern US. *American Journal of Plant*
634 *Sciences* 8. <https://doi.org/10.4236/ajps.2017.86087>

635 Breiman, L., 2001. *Random Forests* (No. 9788578110796). Berkeley, California.
636 <https://doi.org/10.1017/CBO9781107415324.004>

637 Brooks, J.F., 2020. *Winterthur Portfolio*. Henry Francis du Pont Winterthur Museum, Inc. 54, 186–
638 188. <https://doi.org/10.1086/711330>

639 Bünemann, E.K., Bongiorno, G., Bai, Z., Creamer, R.E., De Deyn, G., De Goede, R., Fleskens, L.,
640 Geissen, V., Kuyper, T.W., Mäder, P., Pulleman, M., Sukkel, W., Van Groenigen, J.W.,
641 Brussaard, L., 2018. Soil quality – A critical review. *Soil Biology and Biochemistry* 120, 105–
642 125. <https://doi.org/10.1016/j.soilbio.2018.01.030>

643 Cameron, C.M., 1999. *Hopi dwellings: architectural change at Orayvi*. University of Arizona Press,
644 Tucson.

645 Chadwick, O.A., Chorover, J., 2001. The chemistry of pedogenic thresholds. *Geoderma* 100, 321–
646 353. [https://doi.org/10.1016/S0016-7061\(01\)00027-1](https://doi.org/10.1016/S0016-7061(01)00027-1)

647 Chaney, N.W., Wood, E.F., McBratney, A.B., Hempel, J.W., Nauman, T.W., Brungard, C.W., Odgers,
648 N.P., 2016. POLARIS: A 30-meter probabilistic soil series map of the contiguous United
649 States. *Geoderma* 274, 54–67. <https://doi.org/10.1016/j.geoderma.2016.03.025>

650 Cleveland, D.A., Soleri, D., Smith, S.E., 1994. Do Folk Crop Varieties Have a Role in Sustainable
651 Agriculture? *BioScience* 44, 740–751. <https://doi.org/10.2307/1312583>

652 Costantini, E.A.C., L'Abate, G., 2016. Beyond the concept of dominant soil: Preserving
653 pedodiversity in upscaling soil maps. *Geoderma* 271, 243–253.
654 <https://doi.org/10.1016/j.geoderma.2015.11.024>

655 Damgaard, C., Weiner, J., 2000. DESCRIBING INEQUALITY IN PLANT SIZE OR FECUNDITY. *Ecology*
656 81, 1139–1142. [https://doi.org/10.1890/0012-9658\(2000\)081%255B1139:DIIPSO%255D2.0.CO;2](https://doi.org/10.1890/0012-9658(2000)081%255B1139:DIIPSO%255D2.0.CO;2)

657

658 Dearing, J.A., Wang, R., Zhang, K., Dyke, J.G., Haberl, H., Hossain, Md.S., Langdon, P.G., Lenton,
659 T.M., Raworth, K., Brown, S., Carstensen, J., Cole, M.J., Cornell, S.E., Dawson, T.P.,
660 Doncaster, C.P., Eigenbrod, F., Flörke, M., Jeffers, E., Mackay, A.W., Nykvist, B., Poppy, G.M.,
661 2014. Safe and just operating spaces for regional social-ecological systems. *Global*
662 *Environmental Change* 28, 227–238. <https://doi.org/10.1016/j.gloenvcha.2014.06.012>
663 Dexter, A.R., 2004. Soil physical quality: Part I. Theory, effects of soil texture, density, and organic
664 matter, and effects on root growth. *Geoderma* 120, 201–214.
665 <https://doi.org/10.1016/j.geoderma.2003.09.004>
666 Dominati, E., Patterson, M., Mackay, A., 2010. A framework for classifying and quantifying the
667 natural capital and ecosystem services of soils. *Ecological Economics* 69, 1858–1868.
668 <https://doi.org/10.1016/j.ecolecon.2010.05.002>
669 Dongoske, K.E., Yeatts, M., Anyon, R., Ferguson, T.J., 1997. Archaeological Cultures and Cultural
670 Affiliation: Hopi and Zuni Perspectives in the American Southwest. *Am. antiq.* 62, 600–608.
671 <https://doi.org/10.2307/281880>
672 Doolittle, W.E., 2000. *Cultivated Landscapes of Native North America*. Oxford University
673 Press/Oxford. <https://doi.org/10.1093/oso/9780198234203.001.0001>
674 Dove, D., Di Naso, S., Gutowski, H., Till, J., Tratlener, L., McBride, B. & D., Gerhardt, K., Flink, P.,
675 Dove, D.E., 2006. Topographical Mapping, Geophysical Studies and Archaeological Testing
676 of an Early Pueblo II Village Near Dove Creek, Colorado.
677 <https://doi.org/10.6067/XCV87P8XMQ>
678 Duniway, M.C., Herrick, J.E., Monger, H.C., 2010. Spatial and temporal variability of plant-available
679 water in calcium carbonate-cemented soils and consequences for arid ecosystem
680 resilience. *Oecologia* 163, 215–226. <https://doi.org/10.1007/s00442-009-1530-7>
681 Fadem, C.M., Diederichs, S.R., 2020. Farming the Great Sage Plain: Experimental Agroarchaeology
682 and the Basketmaker III Soil Record. *Culture Agric Food & Envi* 42, 4–15.
683 <https://doi.org/10.1111/cuag.12241>
684 Fath, B.D., Patten, B.C., Choi, J.S., 2001. Complementarity of Ecological Goal Functions. *Journal*
685 *of Theoretical Biology* 208, 493–506. <https://doi.org/10.1006/jtbi.2000.2234>
686 Ferguson, T.J., Colwell-Chanthaphonh, C., 2006. *History Is in the Land: Multivocal Tribal Traditions*
687 *in Arizona's San Pedro Valley*. University of Arizona Press.
688 Gini, C., 1912. *Variabilità e Mulabilità: Contributo allo Studio delle Distribuzioni edelle Relazioni*
689 *Statistiche*. Bologna: Tipografia di Paolo Cuppini.
690 Gorelick, N., Hancher, M., Dixon, M., Ilyushchenko, S., Thau, D., Moore, R., 2017. Google Earth
691 Engine: Planetary-scale geospatial analysis for everyone. *Remote Sensing of Environment*
692 202, 18–27. <https://doi.org/10.1016/j.rse.2017.06.031>
693 Grimm, R., Behrens, T., Märker, M., Elsenbeer, H., 2008. Soil organic carbon concentrations and
694 stocks on Barro Colorado Island — Digital soil mapping using Random Forests analysis.
695 *Geoderma* 146, 102–113. <https://doi.org/10.1016/j.geoderma.2008.05.008>
696 Gustafson, K., Abe, T., 1998. The third boundary condition—was it robin's? *The Mathematical*
697 *Intelligencer* 20, 63–71. <https://doi.org/10.1007/BF03024402>
698 Hack, J., 1942. *The Changing Physical Environment of the Hopi Indians of Arizona*. Cambridge,
699 Mass, Reports of the Awatovi expedition, Peabody museum, Harvard university. Report - no.
700 1, 2.
701 Handayani, I.P., Prawito, P., 2010. Indigenous Soil Knowledge for Sustainable Agriculture, in:
702 Lichtfouse, E. (Ed.), *Sociology, Organic Farming, Climate Change and Soil Science*,

703 Sustainable Agriculture Reviews. Springer Netherlands, Dordrecht, pp. 303–317.
704 https://doi.org/10.1007/978-90-481-3333-8_11

705 Harden, J.W., Taylor, E.M., 1983. A Quantitative Comparison of Soil Development in Four Climatic
706 Regimes. *Quat. res.* 20, 342–359. [https://doi.org/10.1016/0033-5894\(83\)90017-0](https://doi.org/10.1016/0033-5894(83)90017-0)

707 Harris, A., Schoenwetter, J., Warren, A.H., 1960. An Archaeological Survey of the Chuska Valley
708 and Chaco Plateau New Mexico.

709 Hendricks, D.M., 1985. Arizona soils. College of Agriculture, University of Arizona, Tucson, Ariz.

710 Hengl, T., Heuvelink, G.B.M., Stein, A., 2004. A generic framework for spatial prediction of soil
711 variables based on regression-kriging. *Geoderma* 120, 75–93.
712 <https://doi.org/10.1016/j.geoderma.2003.08.018>

713 Hengl, T., Nussbaum, M., Wright, M.N., Heuvelink, G.B.M., Gräler, B., 2018. Random forest as a
714 generic framework for predictive modeling of spatial and spatio-temporal variables. *PeerJ*
715 6, e5518. <https://doi.org/10.7717/peerj.5518>

716 Hopi Department of Natural Resources, 2021. Climate Change Adaptation Plan for the Hopi Tribe.
717 Hopi Office of Community Planning & Economic Development.

718 Horn, R., Taubner, H., Wuttke, M., Baumgartl, T., 1994. Soil physical properties related to soil
719 structure. *Soil and Tillage Research* 30, 187–216. [https://doi.org/10.1016/0167-](https://doi.org/10.1016/0167-720-1987(94)90005-1)
720 [1987\(94\)90005-1](https://doi.org/10.1016/0167-1987(94)90005-1)

721 Huckell, B., 1996. The Archaic Prehistory of the North American Southwest. *Journal of World*
722 *Prehistory* 10, 305–373.

723 Huffman, G., Bolvin, D., Joyce, R., Kelley, O., Nelkin, E., Tan, J., Watters, D., West, J., 2023.
724 Integrated Multi-satellitE Retrievals for GPM (IMERG) Technical Documentation.
725 <https://doi.org/10.5067/GPM/IMERG/3B-MONTH/06>

726 Ibán`ez, J.J., De-Albs, S., Bermúdez, F.F., García-Álvarez, A., 1995. Pedodiversity: concepts and
727 measures. *CATENA* 24, 215–232. [https://doi.org/10.1016/0341-8162\(95\)00028-Q](https://doi.org/10.1016/0341-8162(95)00028-Q)

728 Ibáñez, J.J., Bockheim, J.G. (Eds.), 2013. Pedodiversity, 0 ed. CRC Press.
729 <https://doi.org/10.1201/b14780>

730 Jenny, H., 1941. Factors of Soil Formation: A System of Quantitative Pedology. McGraw- Hill, NY.
731 <https://doi.org/10.2307/211491>

732 Jobbágy, E.G., Jackson, R.B., 2000. THE VERTICAL DISTRIBUTION OF SOIL ORGANIC CARBON AND
733 ITS RELATION TO CLIMATE AND VEGETATION. *Ecological Applications* 10, 423–436.
734 [https://doi.org/10.1890/1051-0761\(2000\)010%255B0423:TVDOSO%255D2.0.CO;2](https://doi.org/10.1890/1051-0761(2000)010%255B0423:TVDOSO%255D2.0.CO;2)

735 Johnson, M.K., Rowe, M.J., Lien, A., López-Hoffman, L., 2021. Enhancing integration of Indigenous
736 agricultural knowledge into USDA Natural Resources Conservation Service cost-share
737 initiatives. *Journal of Soil and Water Conservation* 76, 487–497.
738 <https://doi.org/10.2489/jswc.2021.00179>

739 Johnson, T.E., 2023. The Shifting Nature of Subsistence on the Hopi Indian Reservation.
740 *Agricultural History* 97, 215–244. <https://doi.org/10.1215/00021482-10337941>

741 Jost, L., 2006. Entropy and diversity. *Oikos* 113, 363–375. [https://doi.org/10.1111/j.2006.0030-](https://doi.org/10.1111/j.2006.0030-742-1299.14714.x)
742 [1299.14714.x](https://doi.org/10.1111/j.2006.0030-1299.14714.x)

743 Jury, W.A., Horton, R., 2004. Soil physics, 6. ed. ed. Wiley, Hoboken, NJ.

744 Kahn-John (Diné), M., Koithan, M., 2015. Living in Health, Harmony, and Beauty: The Diné (Navajo)
745 Hózhó Wellness Philosophy. *Glob Adv Health Med* 4, 24–30.
746 <https://doi.org/10.7453/gahmj.2015.044>

747 Kim, H., Møller, I., Thorling, L., Hansen, B., 2025. Sediment color as a predictor of the subsurface
748 redox conditions at large scale. *Applied Geochemistry* 190, 106493.
749 <https://doi.org/10.1016/j.apgeochem.2025.106493>

750 Kimmerer, R., 2013. Braiding Sweetgrass: Indigenous Wisdom, Scientific Knowledge, and the
751 Teachings of Plants. *Environmental Philosophy*.

752 Kohler, T.A., Varien, M.D., Wright, A., Kuckelman, K.A., 2008. Mesa Verde Migrations. *Am. Sci.* 96,
753 146. <https://doi.org/10.1511/2008.70.3641>

754 Laliberté, E., Zemunik, G., Turner, B.L., 2014. Environmental filtering explains variation in plant
755 diversity along resource gradients. *Science* 345, 1602–1605.
756 <https://doi.org/10.1126/science.1256330>

757 Lark, M., 2012. Statistics for Spatio-temporal Data - by Cressie N. & Wikle K.C. *European J Soil*
758 *Science* 63, 534–535. <https://doi.org/10.1111/j.1365-2389.2012.01473.x>

759 Matheron, G., 1963. Principles of geostatistics. *Society of Economic Geologists* 58, 1246-1266-
760 1246–1266. <https://doi.org/10.2113/gsecongeo.58.8.1246>

761 McBratney, A., Minasny, B., 2007. On measuring pedodiversity. *Geoderma* 141, 149–154.
762 <https://doi.org/10.1016/j.geoderma.2007.05.012>

763 McBratney, A.B., De Gruijter, J.J., Brus, D.J., 1992. Spatial prediction and mapping of continuous
764 soil classes. *Geoderma* 54, 39–64. [https://doi.org/10.1016/0016-7061\(92\)90097-Q](https://doi.org/10.1016/0016-7061(92)90097-Q)

765 McBratney, A.B., Santos, M.L.M., Minasny, B., 2003. On digital soil mapping. *Geoderma* 117, 3–
766 52. [https://doi.org/10.1016/S0016-7061\(03\)00223-4](https://doi.org/10.1016/S0016-7061(03)00223-4)

767 McBrinn, M., Cordell, L., 2016. *Archaeology of the Southwest*, Third Edition, 3rd ed. Routledge.
768 <https://doi.org/10.4324/9781315433738>

769 McFadden, L.D., McDonald, E.V., Wells, S.G., Anderson, K., Quade, J., Forman, S.L., 1998. The
770 vesicular layer and carbonate collars of desert soils and pavements: formation, age and
771 relation to climate change. *Geomorphology* 24, 101–145. [https://doi.org/10.1016/S0169-555X\(97\)00095-0](https://doi.org/10.1016/S0169-555X(97)00095-0)

772

773 Meyer, H., Reudenbach, C., Hengl, T., Katurji, M., Nauss, T., 2018. Improving performance of
774 spatio-temporal machine learning models using forward feature selection and target-
775 oriented validation. *Environmental Modelling & Software* 101, 1–9.
776 <https://doi.org/10.1016/j.envsoft.2017.12.001>

777 Mikhailova, E.A., Zurqani, H.A., Post, C.J., Schlautman, M.A., Post, G.C., 2021. Soil Diversity
778 (Pedodiversity) and Ecosystem Services. *Land* 10, 288.
779 <https://doi.org/10.3390/land10030288>

780 Minasny, B., McBratney, A.B., Malone, B.P., Wheeler, I., 2013. Digital Mapping of Soil Carbon, in:
781 *Advances in Agronomy*. Elsevier, pp. 1–47. <https://doi.org/10.1016/B978-0-12-405942-9.00001-3>

782

783 Minasny, B., McBratney, Alex.B., 2016. Digital soil mapping: A brief history and some lessons.
784 *Geoderma* 264, 301–311. <https://doi.org/10.1016/j.geoderma.2015.07.017>

785 Moran, P.A.P., 1950. NOTES ON CONTINUOUS STOCHASTIC PHENOMENA. *Biometrika* 37, 17–23.
786 <https://doi.org/10.1093/biomet/37.1-2.17>

787 Muhs, D.R., 2017. Evaluation of simple geochemical indicators of aeolian sand provenance: Late
788 Quaternary dune fields of North America revisited. *Quaternary Science Reviews* 171, 260–
789 296. <https://doi.org/10.1016/j.quascirev.2017.07.007>

790 Müller, D., Munroe, D.K., 2014. Current and future challenges in land-use science. *Journal of Land*
791 *Use Science* 9, 133–142. <https://doi.org/10.1080/1747423X.2014.883731>

792 Muller, M.R., Munroe, D.K., Batterman, S.A., 2017. Linking biophysical and cultural dimensions of
793 agroecosystems: Biocultural hotspots in North American drylands. *Global Environmental*
794 *Change* 45, 37–49.

795 Nankar, A.N., Pratt, R.C., 2021. Genotyping by Sequencing Reveals Genetic Relatedness of
796 Southwestern U.S. Blue Maize Landraces. *IJMS* 22, 3436.
797 <https://doi.org/10.3390/ijms22073436>

798 Nielsen, D.R., Wendroth, O., 2003. Spatial and temporal statistics: sampling field soils and their
799 vegetation, *GeoEcology Textbook*. Catena-Verl, Reiskirchen.

800 Ortman, S.G., 2016. Uniform Probability Density Analysis and Population History in the Northern
801 Rio Grande. *J Archaeol Method Theory* 23, 95–126. [https://doi.org/10.1007/s10816-014-](https://doi.org/10.1007/s10816-014-9227-6)
802 [9227-6](https://doi.org/10.1007/s10816-014-9227-6)

803 O’Sullivan, R.B., 2003. The Middle Jurassic Entrada Sandstone in northeastern Arizona and
804 adjacent areas, in: *Geology of the Zuni Plateau*. Presented at the 54th Annual Fall Field
805 Conference, New Mexico Geological Society, pp. 303–308. [https://doi.org/10.56577/FFC-](https://doi.org/10.56577/FFC-54.303)
806 [54.303](https://doi.org/10.56577/FFC-54.303)

807 Pawluk, R., 1995. Indigenous knowledge of soil and agriculture at Zuni Pueblo, New Mexico. Iowa
808 State University, Ames, Iowa.

809 Phillips, J.D., 2007. The perfect landscape. *Geomorphology* 84, 159–169.
810 <https://doi.org/10.1016/j.geomorph.2006.01.039>

811 Press, W.H. (Ed.), 2007. *Numerical recipes in Fortran 77: the art of scientific computing*, 2. ed.,
812 repr.corr. to software version 2.10. ed, Fortran numerical recipes. Cambridge University
813 Press, Cambridge.

814 Rao, C.R., 1982. Diversity and dissimilarity coefficients: A unified approach. *Theoretical*
815 *Population Biology* 21, 24–43. [https://doi.org/10.1016/0040-5809\(82\)90004-1](https://doi.org/10.1016/0040-5809(82)90004-1)

816 Rea, A.M., 1997. *At the Desert’s Green Edge: An Ethnobotany of the Gila River Pima*, 1st ed. ed.
817 University of Arizona Press, Erscheinungsort nicht ermittelbar.

818 Redsteer, M.H., Kelley, K.B., Francis, H., Block, D., 2018. Accounts from Tribal Elders: Increasing
819 Vulnerability of the Navajo People to Drought and Climate Change in the Southwestern
820 United States, in: Nakashima, D., Krupnik, I., Rubis, J.T. (Eds.), *Indigenous Knowledge for*
821 *Climate Change Assessment and Adaptation*. Cambridge University Press, pp. 171–187.
822 <https://doi.org/10.1017/9781316481066.013>

823 Reheis, M.C., Goldstein, H.L., Reynolds, R.L., Forman, S.L., Mahan, S.A., Carrara, P.E., 2018. Late
824 Quaternary loess and soils on uplands in the Canyonlands and Mesa Verde areas, Utah and
825 Colorado. *Quat. res.* 89, 718–738. <https://doi.org/10.1017/qua.2017.63>

826 Reneau, S.L., McDonald, E.V., Gardner, J.N., Kolbe, T.R., Carney, J.S., Watt, P.M., Longmire, P.A.,
827 1996. Erosion and deposition on the Pajarito Plateau, New Mexico, and implications for
828 geomorphic responses to late Quaternary climatic changes, in: *The Jemez Mountains*
829 *Region*. Presented at the 47th Annual Fall Field Conference, New Mexico Geological
830 Society, pp. 391–397. <https://doi.org/10.56577/FFC-47.391>

831 Reo, N.J., Whyte, K.P., 2012. Hunting and Morality as Elements of Traditional Ecological Knowledge.
832 *Hum Ecol* 40, 15–27. <https://doi.org/10.1007/s10745-011-9448-1>

833 Rumpel, C., Kögel-Knabner, I., 2011. Deep soil organic matter—a key but poorly understood
834 component of terrestrial C cycle. *Plant Soil* 338, 143–158. [https://doi.org/10.1007/s11104-](https://doi.org/10.1007/s11104-010-0391-5)
835 [010-0391-5](https://doi.org/10.1007/s11104-010-0391-5)

836 Schaetzl, R.J., Anderson, S., 2010. *Soils: genesis and geomorphology*, 4. print. ed. Cambridge Univ.
837 Press, Cambridge.

838 Seager, W.R., Hawley, J.W., Kottowski, F.E., Kelley, S.A., 1987. Geology of east half of Las Cruces
839 and northeast El Paso 1 x 2 sheets, New Mexico. New Mexico Bureau of Geology and Mineral
840 Resources. <https://doi.org/10.58799/GM-57>

841 Sekaquaptewa, E., Washburn, D., 2004. *They Go Along Singing* : Reconstructing the Hopi Past from
842 Ritual Metaphors in Song and Image. *Am. antiq.* 69, 457–486.
843 <https://doi.org/10.2307/4128402>

844 Shannon, C.E., 1948. A Mathematical Theory of Communication. *Bell System Technical Journal* 27,
845 379–423. <https://doi.org/10.1002/j.1538-7305.1948.tb01338.x>

846 Shapiro, S.S., Wilk, M.B., Chen, H.J., 1968. A Comparative Study of Various Tests for Normality.
847 *Journal of the American Statistical Association* 63, 1343–1372.
848 <https://doi.org/10.1080/01621459.1968.10480932>

849 Silverman, B.W., 1986. Density estimation for statistics and data analysis, Monographs on
850 statistics and applied probability. Chapman and Hall, London ; New York.

851 Soleri, D., Cleveland, D., 1993. Hopi crop diversity and change. *Journal of Ethnobiology* 13, 203–
852 231.

853 Stolt, M.H., Ogg, C.M., Baker, J.C., 1994. Strongly Contrasting Redoximorphic Patterns in Virginia
854 Valley and Ridge Paleosols. *Soil Science Soc of Amer J* 58, 477–484.
855 <https://doi.org/10.2136/sssaj1994.03615995005800020033x>

856 Toomanian, N., Esfandiarpour, I., 2010. Challenges of pedodiversity in soil science. *Eurasian Soil*
857 *Sc.* 43, 1486–1502. <https://doi.org/10.1134/S1064229310130089>

858 Torrent, J., Schwertmann, U., Schulze, D.G., 1980. Iron oxide mineralogy of some soils of two river
859 terrace sequences in Spain. *Geoderma* 23, 191–208. [https://doi.org/10.1016/0016-](https://doi.org/10.1016/0016-7061(80)90002-6)
860 [7061\(80\)90002-6](https://doi.org/10.1016/0016-7061(80)90002-6)

861 USGS, 2021. Landsat collection 2.

862 Vivian, R.G., Hilpert, B., 2012. *The Chaco Handbook: An Encyclopedia Guide*. University of Utah
863 Press.

864 Vogel, H.-J., Bartke, S., Daedlow, K., Helming, K., Kögel-Knabner, I., Lang, B., Rabot, E., Russell, D.,
865 Stöbel, B., Weller, U., Wiesmeier, M., Wollschläger, U., 2018. A systemic approach for
866 modeling soil functions. *SOIL* 4, 83–92. <https://doi.org/10.5194/soil-4-83-2018>

867 Wagner, W., Scipal, K., 2000. Large-scale soil moisture mapping in western Africa using the ERS
868 scatterometer. *IEEE Transactions on Geoscience and Remote Sensing* 38, 1777–1782.
869 <https://doi.org/10.1109/36.851761>

870 Walkinshaw, M., 2020. Soil Properties [WWW Document]. California Soil Resource Lab. URL
871 <https://casoilresource.lawr.ucdavis.edu/soil-properties/>

872 Wall, D., Masayesva, V., 2004. People of the Corn: Teachings in Hopi Traditional Agriculture,
873 Spirituality, and Sustainability. *The American Indian Quarterly* 28, 435–453.
874 <https://doi.org/10.1353/aiq.2004.0109>

875 Wallace, Z.P., Nielson, R.M., Stahlecker, D.W., DiDonato, G.T., Ruehmann, M.B., Cole, J., 2021. An
876 abundance estimate of free-roaming horses on the Navajo Nation. *Rangeland Ecology &*
877 *Management* 74, 100–109. <https://doi.org/10.1016/j.rama.2020.10.003>

878 Wang, J.J., 2010. *The Chemistry of Soils*, Second Edition. *Vadose Zone Journal* 9, 198–198.
879 <https://doi.org/10.2136/vzj2009.0141br>

880 Webster, R., Oliver, M.A., 2007. *Geostatistics for Environmental Scientists.*, 2nd ed, Statistics in
881 Practice. John Wiley & Sons, Inc. <https://doi.org/10.2136/vzj2002.0321>

882 Weisiger, M., 2004. The Origins of Navajo Pastoralism. *journal of the Southwest* 46, 253–282.

- 883 Whiteley, P., 2008. Hopi Agriculture and Land Stewardship, in: *Fragile Ecologies: The Nature of*
884 *Nature in Environmental Anthropology*. Routledge, pp. 195–212.
- 885 Whyte, K.P., 2013. On the role of traditional ecological knowledge as a collaborative concept: a
886 philosophical study. *Ecol Process* 2, 7. <https://doi.org/10.1186/2192-1709-2-7>
- 887 Wills, W.H., Drake, B.L., Dorshow, W.B., 2014. Prehistoric deforestation at Chaco Canyon? *Proc*
888 *Natl Acad Sci U S A* 111, 11584–11591. <https://doi.org/10.1073/pnas.1409646111>
- 889 Zhu, A.X., 1997. A similarity model for representing soil spatial information. *Geoderma* 77, 217–
890 242.
- 891